0026-895X/03/6403-600–609$7.00
MOLECULAR PHARMACOLOGY
Copyright © 2003 The American Society for Pharmacology and Experimental Therapeutics
Mol Pharmacol 64:600–609, 2003

Vol. 64, No. 3
2479/1089828
Printed in U.S.A.

Metal-Dependent Inhibition of HIV-1 Integrase by β-Diketo Acids and Resistance of the Soluble Double-Mutant (F185K/C280S)

CHRISTOPHE MARCHAND, ALLISON A. JOHNSON, RAJESHRI G. KARKI, GODWIN C. G. PAIS, XUECHUN ZHANG, KIRIANA COWANSAGE, TAPAN A. PATEL, MARC C. NICKLAUS, TERRENCE R. BURKE, JR., and YVES POMMIER

Laboratory of Molecular Pharmacology, Center for Cancer Research, National Cancer Institute, National Institutes of Health, Bethesda, Maryland (C.M., A.A.J., K.C., T.A.P., Y.P.); and Laboratory of Medicinal Chemistry, Center for Cancer Research, National Cancer Institute, Frederick, Maryland (R.G.K., G.C.G.P., X.Z., M.C.N., T.R.B.)

Received February 24, 2003; accepted May 30, 2003

This article is available online at http://molpharm.aspetjournals.org

ABSTRACT

The β-diketo acids (DKAs) represent a major advance for anti–HIV-1 integrase drug development. We compared the inhibition of HIV-1 integrase by six DKA derivatives using the wild-type enzyme or the double-mutant F185K/C280S, which has been previously used for crystal structure determinations. With the wild-type enzyme, we found that DKAs could be classified into two groups: those similarly potent in the presence of magnesium and manganese and those potent in manganese and relatively ineffective in the presence of magnesium. Both the aromatic and the carboxylic or tetrazole functions of DKAs determined their metal selectivity. The F185K/C280S enzyme was markedly more active in the presence of manganese than magnesium. The F185K/C280S integrase was also relatively resistant to the same group of DKAs that were potent in the presence of magnesium with the wild-type enzyme. Resistance was caused by a synergistic effect from both the F185K and C280S mutations. Molecular modeling and docking suggested metal-dependent differences for binding of DKAs. Molecular modeling also indicated that the tetrazole or the azido groups of some derivatives could directly chelate magnesium or manganese in the integrase catalytic site. Together, these experiments suggest that DKAs recognize conformational differences between wild-type and the double-mutant HIV-1 integrase, because they chelate the magnesium or manganese in the enzyme active site and compete for DNA binding.

Because actual treatments targeting HIV reverse transcriptase and protease do not suppress viral replication in all AIDS patients (Richman, 2001) and because HIV-1 integrase, a viral enzyme encoded by the *pol* gene, is critical for the HIV-1 viral cycle, HIV-1 integrase is a rational target for anti-AIDS therapy [for a recent review, see De Clercq (2001)]. After viral entry and reverse transcription, HIV-1 integrase catalyzes the integration of the viral DNA copies into host cell chromosomes [for reviews, see Pommier et al. (1997); Brown (1998); Skalka (1999)]. In the cytoplasm, integrase catalyzes the 3′-processing (3′-P) step consisting of the removal of a GT dinucleotide from the 3′-end of both extremities of the viral genome [U3 and U5 long terminal repeats (LTRs)] (see Fig. 1A). Then, integrase bound to the LTRs in the preintegration complex (Bowerman et al., 1989; Farnet and Haseltine, 1991; Miller et al., 1997) migrates to the nucleus, where the strand transfer (ST) step of the integration reaction occurs. In this reaction, the 3′-recessed viral ends (donor DNA) attack host chromosomes (acceptor DNA). Completion of the integration process requires excision of the two 5′-unpaired viral nucleotides, and gap filling, which is probably accomplished by cellular enzymes.

Integration can be monitored in vitro using recombinant HIV-1 integrase and a radiolabeled DNA substrate. In this assay, a 21-mer double-stranded DNA oligonucleotide corresponding to the last 21 base pairs of the U5 viral LTRs (Fig. 1A) is used as substrate to follow both the 3′-P and the ST reactions. 3′-P generates a 19-mer product, which can be integrated in another 21-mer double-stranded DNA oligonucleotide substrate during ST (Fig. 1A). Integration can occur at different positions on the acceptor DNA molecule, leading to several products migrating slower and faster than the original 21-mer substrate. Higher molecular weight species (Fig. 1B) can be used to quantify ST products [for review, see Marchand et al. (2001)].

β-Diketo acids (DKAs) are the first antiviral HIV-1 integrase inhibitors reported to be highly specific for integrase (Goldgur et al., 1999; Hazuda et al., 2000). Two DKAs are

ABBREVIATIONS: 3′-P, 3′-processing; ST, strand transfer; DKA, β-diketo acids; MOPS, 3-(*N*-morpholino)propanesulfonic acid; 5CITEP, 1-(5-chloroindol-3-yl)-3-(tetrazolyl)-1,3-propanedione enol; L-708,906, 4-[3,5-bis(benzyloxy)phenyl]-2-hydroxy-4-oxobut-2-enoic acid; DA-DKA, diazido β-diketo acids; MA-DKA, mono-azido β-diketo acids; LTRs, long terminal repeats.

currently in clinical trial (Yoshinaga et al., 2002; Young et al., 2002; Billich, 2003) [for review, see Billich (2003); Johnson et al. (2003)]. In vitro, DKAs inhibit integration by selectively blocking ST (Hazuda et al., 2000; Marchand et al., 2002). DKAs have been proposed to bind to a divalent metal ion in the integrase catalytic site (Grobler et al., 2002; Pais et al., 2002) and this binding is metal dependent (Grobler et al., 2002).

In vitro, the wild-type HIV-1 integrase requires manganese (Mn^{2+}) or magnesium (Mg^{2+}) for activity (Engelman and Craigie, 1995; Deprez et al., 2000; Leh et al., 2000). In 12 of the studies published in 2003 using recombinant retroviral integrases, four were performed with Mg^{2+} as a divalent metal cofactor (Cherepanov et al., 2003; Singh et al., 2003a,b; Zhuang et al., 2003), whereas five studies used Mn^{2+} (Bao et al., 2003; Priet et al., 2003; Zagarian et al., 2003; Zhang et al., 2003; Zhao et al., 2003). Three other studies were performed with Mg^{2+} as well as Mn^{2+} (Bischerour et al., 2003; King et al., 2003; Podtelezhnikov et al., 2003). Thus, there is no consensus on the metal to be used for in vitro integrase catalytic assays. In addition, the relevant metal used by HIV-1 integrase in vivo still remains to be identified. Therefore, the initial aim of the present study was to investigate the metal and DKA structure requirements for HIV-1 integrase inhibition by a series of structurally different DKAs.

A double-mutant of HIV-1 integrase bearing two mutations, F185K and C280S, was designed to improve the enzyme solubility for crystallization purposes (Jenkins et al., 1996). This enzyme has been reported to be as catalytically active as the wild-type enzyme in vitro (Jenkins et al., 1996). The mutation F185K is localized in the enzyme core domain at the dimer interface (i.e., located on the surface of one monomer that contacts another monomer) and is present in all crystal structures (Dyda et al., 1994; Goldgur et al., 1998, 1999; Maignan et al., 1998; Chen et al., 2000a; Wang et al., 2001). The mutation F185K is deleterious to virion assembly in vivo (Jenkins et al., 1996) and decreases the in vitro activity of the enzyme in the presence of Mg^{2+} (Podtelezhnikov et al., 2003). The mutation C280S is located in the enzyme C-terminal domain and is present in the crystal structure involving both core and C-terminal domains (Chen et al., 2000a). This mutation abolishes the disulfide-related oligomerization of integrase but does not affect viral replication as well as in vitro catalytic activity (Bischerour et al., 2003).

We studied the potency of a series of DKAs for inhibition of the wild-type enzyme in the presence of Mn^{2+} and Mg^{2+} and compared the results with those obtained using the double-mutant F185K/C280S enzyme in the presence of Mn^{2+} (Marchand et al., 2002). We report that the selected DKAs exhibit different metal requirements for the inhibition of the wild-type enzyme and that these differences are determined both by the aromatic and the acidic portions of the DKAs. Molecular modeling was performed to interpret these observations. We also found that the double-mutant integrase is relatively resistant to some of the DKAs, suggesting that caution should be used in the interpretation of structural studies involving mutations F185K and C280S, as well as inhibition data obtained with this integrase mutant.

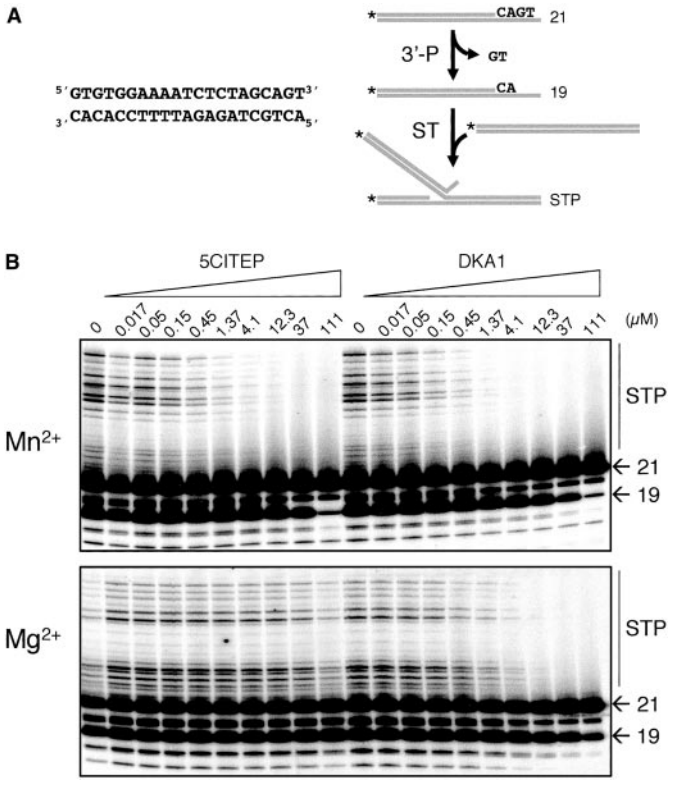

Fig. 1. Comparison of HIV-1 integrase inhibition by 5CITEP and DKA1 in the presence of Mn^{2+} and Mg^{2+}. A, sequence of the double-stranded oligonucleotide used as substrate and schematic representation of the in vitro integration assay. The ^{32}P–end-labeled oligonucleotide substrate can be integrated into itself during the two steps of the integration reaction. B, PhosphorImager image showing a typical experiment performed in the presence of Mn^{2+}. 21, 19, and STP correspond to the DNA substrate, the 3′-processing product, and the strand transfer products, respectively. C, PhosphorImager image showing a typical experiment performed in the presence of Mg^{2+}.

Materials and Methods

DNA Oligonucleotides and Drugs. Oligonucleotides were purchased from IDT Inc. (Coralville, IA) and purified on 20% (19:1) denaturing polyacrylamide gels using UV shadow. Purified oligonucleotides were 5′-end labeled by T4-polynucleotide kinase (New England Biolabs, Inc. Beverly, MA) as described previously (Marchand et al., 2001). The synthesis of DKA derivatives has been described in detail separately (Pais et al., 2002; Zhang et al., 2002).

HIV-1 Integrase Expression and Purification. The double-mutant F185K/C280S integrase was expressed and purified as described previously (Marchand et al., 2001). The wild-type enzyme was expressed and purified accordingly with the following modifications: 10% glycerol was added to all the purification buffers and 50 μM of $ZnCl_2$ was added to the elution buffer (25 mM HEPES, pH 6.7, 0.5 M NaCl, 2 mM β-mercaptoethanol, and 750 mM of imidazole) (Leh et al., 2000). Dialysis was performed in a buffer containing 50 mM HEPES, pH 6.7, 1 M NaCl, 4 mM EDTA, 2 mM dithiothreitol, and 50% glycerol.

HIV-1 Integrase Site Mutagenesis. F185K and C280S single-mutants were generated using the QuikChange site-directed mutagenesis kit (Stratagene, La Jolla, CA), according to the manufacturer's recommendations. Two sets of oligonucleotides, F185K$^+$ (34-mer, 5′-GGCAGTATTCATCCACAATAAAAAAAGAAAAGGG-3′), F185K$^-$ (34-mer, 5′-CCCTTTTCTTTTTTTATTGTGGATGAATACTGCC-3′) and C280S$^+$ (27-mer, 5′-GGCAGGTGATGATAGTGTGGCAAGTAG-3′), C280S$^-$ (27-mer, 5′-CTACTTGCCACACTATCATCACCTGCC-3′) embedding the 185 and 280 mutations, respectively, were purchased from IDT (Coralville, IL). Polymerase chain reaction was performed with each set of primers and the pET-15b-IN$^{1-288}$ plasmid (Engelman and Craigie, 1992) as a start-

ing template. Mutants were selected by sequencing and were used for protein expression as described above.

HIV-1 Integrase Inhibition Assay. The HIV-1 integrase assays were performed as described previously (Marchand et al., 2002). Briefly, the integrase-DNA complexes were preformed (Hazuda et al., 1994) by mixing 400 nM of HIV-1 integrase with 20 nM concentrations of the 5′-end ^{32}P-labeled, 21-mer, double-stranded DNA template for 15 min on ice in a reaction buffer containing 25 mM MOPS, pH 7.2, 50 mM NaCl, 7.5 mM $MnCl_2$ or $MgCl_2$, and 14.3 mM β-mercaptoethanol. Inhibitors were then added to reactions in a final volume of 10 μl, and integration reactions were carried out for 1 h at 37°C. Reactions were quenched by adding 10 μl of denaturing loading dye (99% formamide, 1% SDS, 0.2 mg/ml bromphenol blue, and 0.2 mg/ml xylene cyanol). Samples were loaded onto 20% (19:1) denaturing polyacrylamide gels. Gels were dried, exposed overnight and analyzed using a PhosphorImager (Amersham Biosciences, Piscataway, NJ). The densitometric analysis was performed using ImageQuant (Amersham Biosciences). Each lane was quantified for 3′-P and ST products, which were expressed as a fraction of the total DNA per lane. Percentage of inhibition was computed using the integrase control lanes as a reference.

Molecular Modeling and Docking Studies. Docking studies were performed on the structural model of the full-length HIV-1 integrase complexed with donor DNA using the program GLIDE, part of the First Discovery suite (Schrödinger Inc., Portland, OR). The coordinates of the full-length HIV-1 integrase tetramer complexed with donor and acceptor DNA were the results of modeling, using all available experimental evidence (Karki et al., 2002). Known crystal structures (Lodi et al., 1995; Cai et al., 1997; Maignan et al., 1998; Goldgur et al., 1999; Chen et al., 2000a; Wang et al., 2001) were used as templates for structure building. All missing residues were added using the Biopolymer module in Sybyl 6.8 (Tripos Inc., St. Louis, MO), and the conformation was adjusted by the loop search method. The whole complex was refined by molecular dynamics simulation using the program CHARMM (Brooks et al., 1983), version c27b3, with the CHARMM all-atom force field (MacKerell et al., 1998; Foloppe and MacKerell, 2000) in vacuo followed by molecular dynamics simulation in a 10-Å shell of explicit solvent. The transferable intermolecular potential-3-point water model was used to simulate the solvent (Jorgensen et al., 1983). Each monomer consists of residues 1 to 288. This structural model shows differences from models reported earlier (Heuer and Brown, 1998; Chen et al.,

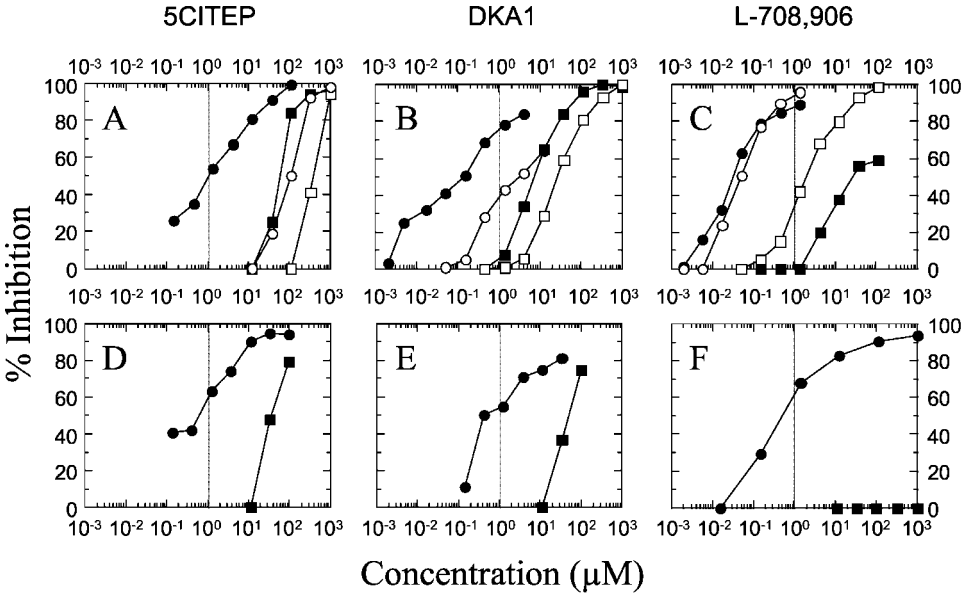

Fig. 2. HIV-1 integrase inhibition curves (derived from densitometric analysis of typical experiments) for 5CITEP, its carboxylate analog DKA1, and L-708,906. Graphs represent the percentage of inhibition for the two integration steps as a function of the drug concentration. Circles, inhibition of strand transfer; squares, inhibition of 3′-processing; filled symbols, Mn^{2+}; open symbols, Mg^{2+}. A, B, and C, wild-type integrase; D, E, and F, double-mutant F185K/C280S integrase.

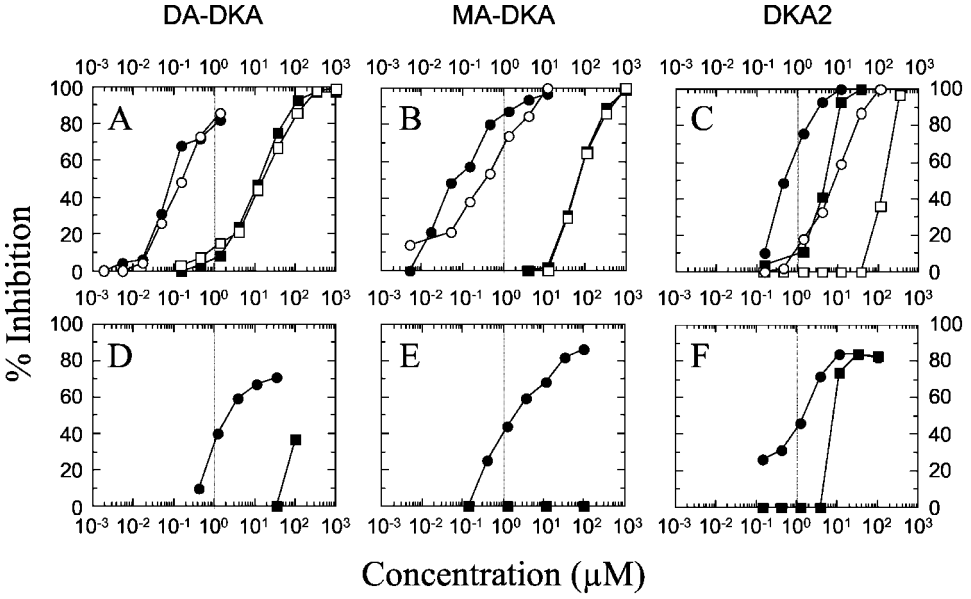

Fig. 3. HIV-1 integrase inhibition curves (derived from densitometric analysis of typical experiments) for azido-containing DKAs (DA-DKA and MA-DKA) and the bifunctional DKA2. Graphs represent the percentage of inhibition for the two integration steps as a function of the drug concentration. Circles, inhibition of strand transfer; squares, inhibition of 3′-processing; filled symbols, Mn^{2+}; open symbols, Mg^{2+}. A, B, and C, wild-type integrase; D, E, and F, double-mutant F185K/C280S integrase.

2000a,b; Gao et al., 2001; Podtelezhnikov et al., 2003), and a detailed account will be published elsewhere. For the purpose of this study, a dimer of the full-length integrase complexed with donor DNA was extracted from the modeled tetramer complex. This structural model was refined further by running a series of restrained impact energy minimizations using the Impact utility, part of the first discovery suite (Schrödinger Inc., Portland, OR), until the average root-mean-square deviation of the nonhydrogen atoms reached 0.3 Å. Grid files representing shape and properties of the receptor were generated separately, with either Mg^{2+} or Mn^{2+} in the active site, respectively. The three-dimensional structures of the inhibitors used for docking were constructed using the 3D-Sketcher tool available through the Maestro interface of the program GLIDE. The geometry of the structures was optimized using the OPLS-AA force field (Jorgensen et al., 1996) to perform 1000 steps of conjugate gradient minimization. The optimized structures were then docked using the precomputed grid files; for each of them, 100 poses were saved.

Results

Because DKAs have been proposed to bind a divalent metal ion in the catalytic site of the enzyme (Grobler et al., 2002; Pais et al., 2002) in a metal-dependent manner (Grobler et al., 2002), we studied the potency of DKAs for the in vitro inhibition of wild-type integrase in the presence of Mn^{2+} versus Mg^{2+} and compared the effects of DKAs against the wild-type and the soluble double-mutant enzymes (Marchand et al., 2002). Even though the double-mutant has been reported to be active in the presence of Mg^{2+} (Jenkins et al., 1996), we found in our laboratory that the activity level of the double–mutant in the presence Mg^{2+} was not suitable for inhibitor testing. In the presence of Mn^{2+}, the catalytic activity of the double-mutant enzyme was equivalent to that of wild-type integrase (Marchand et al., 2002). The drug inhibition data are shown as dose response curves in Figs. 2 and 3, and IC_{50} values are summarized in Table 1.

The Carboxylic Function Enhances Inhibition of Wild-Type Integrase in the Presence of Mg^{2+}. To study the metal selectivity for inhibition of wild-type HIV-1 integrase by DKAs, we compared the activity of 5CITEP and DKA1, bearing a carboxylic function compared with the tetrazole group (Table 1) (Goldgur et al., 1999; Pais et al., 2002). We previously reported these two inhibitors to be equivalent for inhibition of the double-mutant integrase in the presence of Mn^{2+} (Marchand et al., 2002), but they were recently described to exhibit differential binding efficiencies depending on the metal present in the reaction (Grobler et al., 2002). Using wild-type HIV-1 integrase, 5CITEP inhibited ST in the

TABLE 1
Summary of IC_{50} values for the compounds tested

Compound	Structure	Reaction	In Vitro IC_{50} Values				
			Wild-Type			Double Mutant	
			$MgCl_2$	$MnCl_2$	Mn/Mg	$MnCl_2$	DM/WT
					μM		
L-708,906	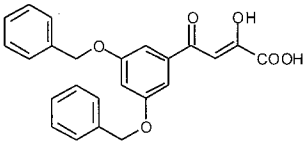	ST 3′-P	0.06 ± 0.01^a 1.9, 3.0[c]	0.06 ± 0.01^b 27, 18[c]	1	0.42 ± 0.08^b >1000	7
DA-DKA	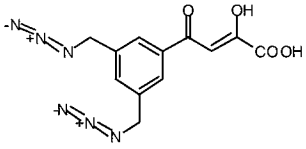	ST 3′-P	0.46 ± 0.08^a 17, 32[c]	0.08 ± 0.01^a 13, 27[c]	0.17	2.0, 2.8[c] >100	30
MA-DKA	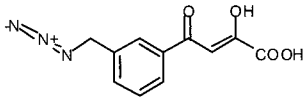	ST 3′-P	0.33 ± 0.03^a 70, 90[c]	0.07 ± 0.01^a 70, 110[c]	0.21	1.53 ± 0.27^a >100	22
DKA2	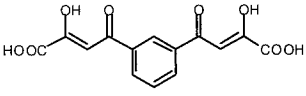	ST 3′-P	8.2, 12[a] 150, 70[c]	0.45, 0.75[c] 4.8, 5.5[c]	0.06	1.83 ± 032^a 7.87 ± 2.25^a	3
DKA1	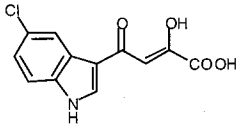	ST 3′-P	1.93 ± 0.93^a 25, 30[c]	0.12 ± 0.04^a 7, 15[c]	0.06	0.52 ± 0.10^a 48, 80[c]	4
5CITEP	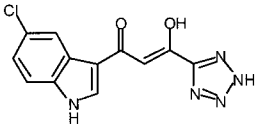	ST 3′-P	97 ± 32^a 400, >333[c]	0.93 ± 0.23^a 59, 40[c]	0.01	0.65 ± 0.19^a 35, 70[c]	0.7

[a] Three independent experiments.
[b] Four independent experiments.
[c] Two independent experiments.

presence of Mn^{2+} (Figs. 1B, top gel, and 2A) with an IC_{50} value of 0.93 μM (Table 1) but was approximately 100-fold less active in the presence of Mg^{2+} (Figs. 1B, bottom gel, and 2A; Table 1). DKA1 was more potent than 5CITEP in the presence of Mn^{2+} (Figs. 1B, top gel, and 2B; Table 1) and was even more potent than 5CITEP in the presence of Mg^{2+} (Figs. 1B, bottom gel, and 2B; Table 1). Thus our data confirm that the tetrazole and carboxylic functions are not equivalent for inhibition of the wild-type integrase (Grobler et al., 2002). The lack of potency of 5CITEP in the presence of Mg^{2+} may be explained by the reduced binding of the tetrazole group in the catalytic site of the enzyme in the presence of Mg^{2+} (Grobler et al., 2002). Together, these results demonstrate that potent inhibition of wild-type integrase in the presence of Mg^{2+} requires a carboxylic function rather than a tetrazole in the DKAs.

The Carboxylic Group Increases Selectivity for the Wild-Type Enzyme. Figure 2 demonstrates that in the presence of Mn^{2+}, the potency of 5CITEP for ST was almost equivalent against the wild-type and the double-mutant enzymes (compare Fig. 2, A and D). By contrast, DKA1, which is also a Mn^{2+}-selective drug (Fig. 2B), was more potent against the wild-type enzyme than the double mutant when tested in the presence of Mn^{2+} (compare Fig. 2, B and E). These results demonstrate that the carboxylic group is not only required for potency in the presence of Mg^{2+} but is also globally more efficient than the tetrazole function for inhibition of the wild-type enzyme.

The Aromatic Portion of DKAs Contributes to the Metal Selective Inhibition of HIV-1 Integrase. To evaluate the influence of the aromatic portion of DKAs, we also tested the Merck compound L-708,906 (Table 1), which differs from DKA1 by the replacement of the chloro-indole group with a bis-benzyloxy phenyl group (see Table 1). With the wild-type enzyme, L-708,906 showed the same IC_{50} value of 0.06 μM for ST inhibition with either Mg^{2+} or Mn^{2+} (Fig. 2C; Table 1). Thus, exchanging the chloro-indole group of DKA1 for the bis-benzyloxy phenyl group of L-708,906 selectively increased potency against ST in the presence of Mg^{2+} (30-fold; 1.93 versus 0.06 μM) compared with Mn^{2+} (2-fold; 0.12 versus 0.06 μM) (Table 1). Moreover, the potency of L-708,906 in the 3′-P reaction was 6- to 14-fold greater in the presence of Mg^{2+} than in the presence of Mn^{2+} (Fig. 2C, Table 1). The nitrogen atom present in the indole ring of DKA1 does not play any significant role in the metal selectivity because a naphthalene-containing DKA lacking this nitrogen was also Mn^{2+}-selective (data not shown). DKA1 is more potent in the presence of Mn^{2+}, whereas L-708,906 is equally active for ST with either Mg^{2+} or Mn^{2+} and more potent for 3′-P in the presence of Mg^{2+} than Mn^{2+}, which demonstrates that the structure of the aromatic moiety of the DKAs contributes to their metal selectivity.

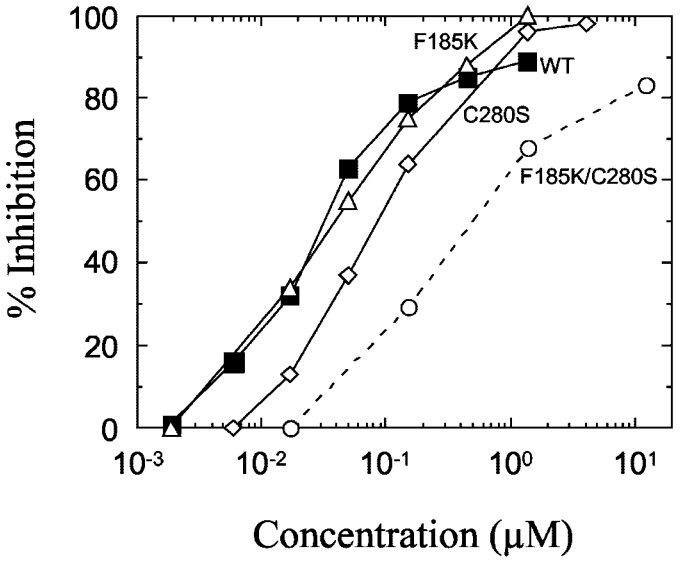

Fig. 4. Resistance of HIV-1 mutant integrases to L-708,906. The graph corresponds to the densitometric analysis of a typical experiment and represents the percentage of inhibition of strand transfer as a function of drug concentration. ■, inhibition of wild-type integrase; ○, F185K/C280S double-mutant; △, F185K single-mutant; ◇, C280S single-mutant.

The Aromatic Portion of DKAs Can Be Modified without Abrogating Mg^{2+}-Dependent Inhibition of HIV-1 Integrase. To further investigate the influence of the aromatic portion of DKAs for their metal selectivity, we extended our studies to the novel azido-containing DKAs (Table 1). We previously reported that these compounds are selective inhibitors of ST, with potency similar to that of L-708,906 in assays using the double-mutant integrase (Zhang et al., 2002). Figure 3 shows that the di-azido DKA (DA-DKA) and the mono-azido DKA (MA-DKA) exhibit potency similar to that of L-708,906 when tested with the wild-type enzyme in the presence of Mn^{2+} (Fig. 2C, Table 1). They also exhibit submicromolar IC_{50} values for ST inhibition in the presence of Mg^{2+}. DA-DKA and MA-DKA were also 20- to 30-fold less potent when tested against the double-mutant in the presence of Mn^{2+} (Fig. 3, D and E). These results demonstrate that the aromatic portion of L-708,906 can be modified while retaining the activity of these compounds with either Mg^{2+} or Mn^{2+}.

A Second Diketo Acid Side Chain on the Central Aromatic Ring Confers Mn^{2+} Selectivity. We reported previously that the bifunctional DKA (DKA2) (Table 1), which contains a second diketo acid side chain appended to the central aromatic ring, is more efficient for 3′-P inhibition than DKAs with a single diketo function, when tested against the double-mutant integrase in the presence of Mn^{2+} (Marchand et al., 2002) (Fig. 3F). When tested against the wild-type enzyme, DKA2 showed weaker inhibition in the presence of Mg^{2+} than Mn^{2+} (Fig. 3C), as was observed for 5CITEP and DKA1 (Fig. 2). The IC_{50} values of DKA2 for ST/3′-P in the presence of Mn^{2+} and Mg^{2+} were approximately 0.6/5 and 10/110 μM, respectively (Fig. 3C, Table 1). These experiments indicate that the introduction of a second diketo acid side chain in the DKA2 molecule, rendering it symmetrical, reduces potency, especially in the presence of Mg^{2+} compared with the other DKAs: L-708,906, DA-DKA, and MA-DKA. In the presence of Mn^{2+}, DKA2 had almost equivalent potency against wild-type (Fig. 3C) and double-mutant enzymes (Fig. 3F). Thus, among the DKAs examined, DKA2, DKA1, and 5CITEP (see Fig. 2) showed similar activity in the double-mutant and wild-type integrases.

The Double-Mutant Integrase Is Resistant to L-708,906 and the Azido-Containing DKAs. Fig. 2, C and F, shows that L-708,906 is more potent against wild-type integrase than the double-mutant by approximately 40-fold for 3′-P and 7-fold for ST (Table 1). Similarly, we found that the azido-containing DKAs (DA-DKA and MA-DKA) were markedly more potent against the wild-type integrase than

the double mutant. The double mutant is thus relatively resistant to L-708,906 and to the azido-containing DKAs. These experiments demonstrate that the DKAs studied fall into two groups. The first group (L-708,906, DA-DKA, and MA-DKA) shows resistance in the double-mutant enzyme; and the second group (5CITEP, DKA1, and DKA2) has comparable activities against both enzymes.

The ability of wild-type enzyme to discriminate for ST between these two groups of compounds, given that all of them had similar activity against the double-mutant enzyme, suggests that structural differences between the wild-type and the double-mutant integrases are recognized by the DKAs.

Mutations F185K and C280S Have a Synergistic Effect on the Resistance of the Double-Mutant Integrase to L-708,906. To determine the effect of each mutation on the resistance to DKAs of the double-mutant integrase, we expressed single-mutant proteins bearing either the F185K or the C280S mutation and tested L-708,906 against each of these mutant enzymes in the presence of Mn^{2+}. These two single mutant proteins had similar catalytic activities compared with the wild-type enzyme (data not shown). The ST inhibition curves are presented in Fig. 4. The inhibition curve of the F185K mutant is almost superimposable upon the one of the wild-type enzyme (Fig. 4), suggesting that this mutation alone cannot be held responsible for the observed resistance of the double-mutant to L-708,906. The C280S mutant was more resistant to L-708,906 than the wild-type enzyme, but this resistance was almost 10-fold lower than that of the double-mutant. These experiments demonstrate that the resistance observed with the double-mutant integrase is caused by a synergistic effect of both the F185K and the C280S mutations.

Molecular Modeling and Docking Studies. Molecular modeling was performed by docking the various inhibitors into a structural model of full-length HIV-1 integrase dimer complexed with donor DNA. DKAs can bind in the catalytic site of HIV-1 integrase in the absence of DNA substrate as shown by the crystal structure of 5CITEP with the enzyme core domain (Goldgur et al., 1999). Resistance mutations to DKAs are located in the enzyme active site in the vicinity of catalytic residues D64, D116, and E152 (Hazuda et al., 2000;

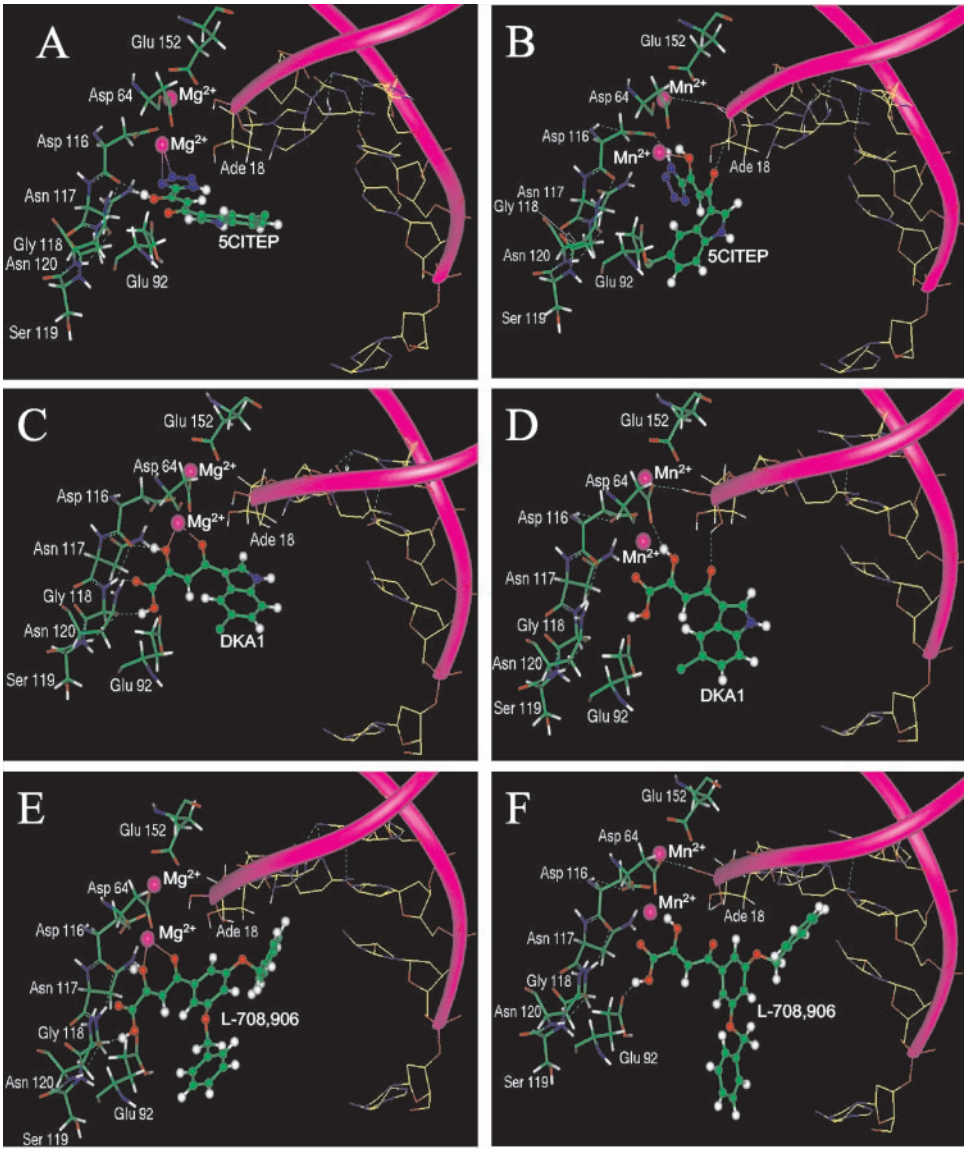

Fig. 5. Docking models of 5CITEP, DKA1, and L-708906 in the presence of Mg^{2+} and Mn^{2+}, obtained using GLIDE. Hydrogen bonds are represented as dashed lines in green and interactions with the metal ions are in magenta. For clarity reasons, only important residues and atoms are shown. A, C, and E, Mg^{2+}; B, D, and F, Mn^{2+}.

Witvrouw et al., 2002) [for reviews, see Neamati (2002); Johnson et al. (2003)]. It has been speculated that HIV-1 integrase could require binding of two divalent metal ions in its active site to achieve integration and that DKAs inhibit integrase via sequestration of these metals (Grobler et al., 2002; Pais et al., 2002).

Figure 5 shows differences in the binding of 5CITEP and DKA1 in the presence of Mg^{2+} (Fig. 5, A and C). DKA1 chelates one of the Mg^{2+} ions by its diketo group and interacts via hydrogen bonding of its carboxylic group with Asn120 and Gly118 (Fig. 5C). On the other hand, 5CITEP interacts with the divalent metal via its tetrazole group and binds in a different orientation (Fig. 5A). This orientation is slightly different from the one observed in the crystal structure (Goldgur et al., 1999), which may be related to crystallographic environment (crystal packing). Thus, 5CITEP could retain considerable mobility and adopt different orientations in the binding site of integrase (Sotriffer et al., 2000a,b). In the case of DKA1, our model suggests that the presence of the carboxylic acid group could provide an optimal positioning of the diketo group for chelation of the divalent metal, which globally would increase binding efficiency of the drug. In the presence of Mn^{2+}, the binding of 5CITEP and DKA1 are more similar (Fig. 5, B and D) and the hydrogen bonding with the enzyme is now brought about by the tetrazole hydrogen in the case of 5CITEP and the enolic hydroxy group in case of DKA1.

L-708,906 adopts an orientation similar to that of DKA1 in the presence of Mg^{2+} or Mn^{2+} (Fig. 5, E and F). For these two carboxylate-containing compounds, the chelation of the Mg^{2+} metal ion is performed by the two planar oxygens of the diketo function, whereas the chelation of Mn^{2+} is shared by one oxygen of the carboxylate and one of the diketo function (compare Fig. 5, C and E with D and F). The sliding of the molecule toward the carboxylate in the presence of Mn^{2+} could be explained by the existence of a slightly more flexible coordination sphere for Mn^{2+} than for Mg^{2+} (Bock et al., 1999). Moreover, L-708,906 fills the catalytic pocket more efficiently with its aromatic portion than DKA1 (compare Fig. 5, C and D with E and F). One aromatic arm of L-708,906 reaches and interacts with the donor DNA, which may increase binding efficiency. Biochemical experiments also suggest an interaction between DKAs and the terminal unpaired

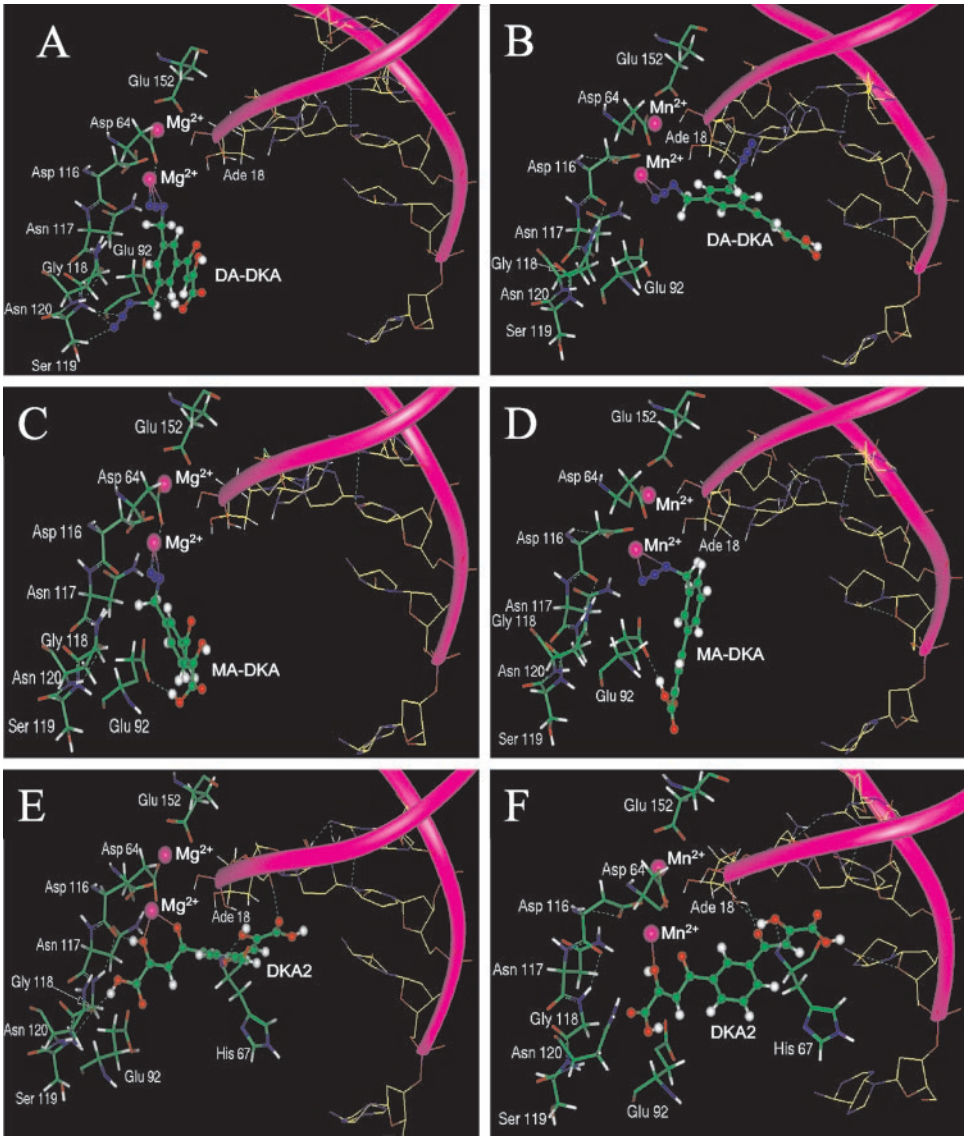

Fig. 6. Docking models of DA-DKA, MA-DKA, and DKA2 in the presence of Mg^{2+} and Mn^{2+}, obtained using GLIDE. Hydrogen bonds are represented as dashed lines in green and interactions with the metal ions are in magenta. For clarity reasons, only important residues and atoms are shown. A, C, and E, Mg^{2+}; B, D, and F, Mn^{2+}.

dinucleotide present in the donor DNA (Marchand et al., 2002).

The docking of the azido-containing DKAs reveals that DA-DKA and MA-DKA could bind in two optimal orientations. One is similar to DKA1 and L-708,906 (not shown). Surprisingly, in the other orientation (shown in Fig. 6, A and D), the diketo groups do not participate in divalent metal chelation. The chelation is instead performed by one of the azido arms, and the orientation of the azido-containing DKAs is metal selective (compare Fig. 6, A and C with B and D; note the orientation of the diketo group). A search of the Cambridge Structural Database (CSD version 5.23) (Allen and Kennard, 1993) for organic compounds containing nitrogen and magnesium using the program Quest (version 5) resulted in 321 hits for which nitrogens chelate the metal ion (data not shown). This suggests that an azido group can potentially replace the diketo acid side chain of the DKA as the chelating moiety.

The docking of the bifunctional DKA2 indicates an interaction of the diketo group of one side chain with the divalent cation (Fig. 6, E and F) and suggests a conservation of the orientation of the molecule in the presence of either Mg^{2+} or Mn^{2+}. Our molecular modeling and docking studies demonstrate the importance of the DKAs' carboxylic function for Mg^{2+} chelation by the diketo group of DKAs. They also suggest that DKAs bind to the active site of integrase differentially in the presence of Mg^{2+} and Mn^{2+}. Finally, they reveal a potential chelation of either the Mg^{2+} or Mn^{2+} by the azido group of the azido-containing DKAs and by the tetrazole of 5CITEP.

Discussion

The potency of DKAs against wild-type HIV-1 integrase is divalent metal-dependent (Grobler et al., 2002; current study). The present study further demonstrates that this metal-dependence depends on the chemical structure of DKAs (Grobler et al., 2002). Novel azido-containing DKAs (MA-DKA and DA-DKA) and the Merck derivative L-708,906 show almost similar inhibition in the presence of either metal, primarily because these compounds exhibit potent inhibition in the presence of Mg^{2+}. On the other hand, some DKAs, such as 5CITEP, DKA1, or DKA2, are markedly less potent in the presence of Mg^{2+} than Mn^{2+}. We find that both the aromatic and acidic portions of the DKAs contribute to their metal selectivity. In the set of compounds examined, a single carboxylic acid function was required for potency in the presence of Mg^{2+}. Molecular docking demonstrated differences in drug binding in the presence of Mg^{2+} versus Mn^{2+}; the most striking difference was observed with 5CITEP. We also found that metal chelation can involve not only the diketo function but also the nitrogens contained in the azido DKAs or the tetrazole of 5CITEP.

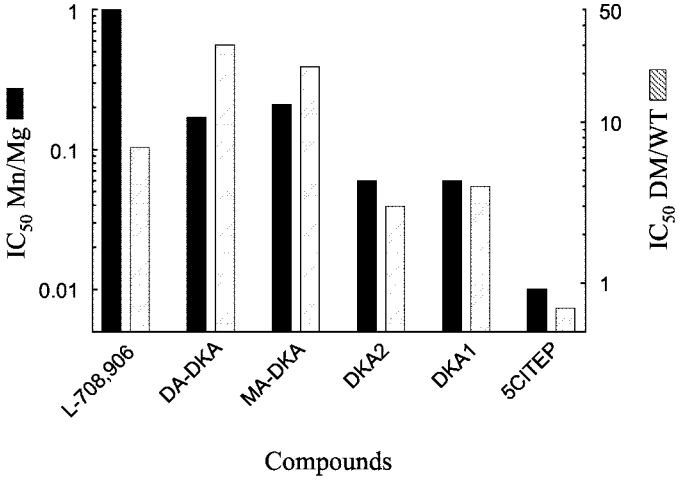

Fig. 7. Correlation between relative activity in magnesium and relative activity against wild-type enzyme. Shown are the ratio of the IC_{50} values for ST obtained in the presence of Mn^{2+} over Mg^{2+} using the wild-type integrase (■, left *y*-axis) and the ratio of the IC_{50} values for ST obtained using the double mutant over the wild-type integrase in the presence of Mn^{2+} (▨, right *y*-axis).

The double-mutant F185K/C280S and the wild-type enzymes are not equivalent for inhibition by some of the DKAs. The double-mutant integrase was resistant to L-708,906 and the two azido DKAs, whereas 5CITEP, DKA1, and DKA2 were similarly active against the two enzymes. This resistance was caused by a synergistic effect of both mutations. The relative potency of the compounds against the wild-type enzyme versus the double-mutant can be expressed as the ratio of the ST IC_{50} values of the double-mutant compared with those obtained with the wild-type enzyme (Table 1, Fig. 7). Figure 7 shows that the selectivity of a given compound for the wild-type enzyme (versus the double-mutant) is directly correlated with the relative activity of that compound in the presence of Mg^{2+} (versus Mn^{2+}). For example, compounds such as L-708,906 or the azido-containing DKAs (DA-DKA and MA-DKA) that are selective for the wild-type enzyme are also potent in the presence of either metal. Conversely, 5CITEP, DKA1, and DKA2 show no cross-resistance against the double-mutant integrase and are relatively inactive against the wild-type integrase in the presence of Mg^{2+}. The differences in drug sensitivity may be caused by structural differences between the integration complexes formed by the wild-type and the double-mutant enzymes. These differences could involve the enzyme active site because we find that the double-mutant integrase requires Mn^{2+} rather than Mg^{2+} for 3′-P and ST activities and because it has been speculated that the active site of integrase is considerably less "tight" in the presence of Mn^{2+} (Esposito and Craigie, 1998). The Mg^{2+}- and wild-type enzyme-selective compounds such as L-708,906 and the azido-containing DKAs may bind preferentially to the enzyme active site in its wild-type configuration in the presence of Mg^{2+}. By contrast, DKA1, DKA2, and 5CITEP may bind poorly to the normal enzyme catalytic site in the presence of Mg^{2+}. The versatility of the Mn^{2+} coordination chemistry (Bock et al., 1999) might allow chelation of DKA1, DKA2, or 5CITEP. Thus, DKAs reveal themselves as molecular probes for differences in the structures of integrase-DNA complexes formed by wild-type and mutant integrase.

The correlation observed between relative drug potency in the presence of Mg^{2+} and relative potency in the wild-type enzyme suggests that assays performed using wild-type enzyme and Mg^{2+} represent the most stringent conditions with respect to drug inhibition. Wild-type integrase in the presence of Mg^{2+} gives the greatest discrimination among DKAs. The ST IC_{50} values range from 0.06 μM for L-708,906 to 97 μM for 5CITEP (Table 1). DKAs may not be the only family of drugs that show a differential potency between wild-type and double-mutant integrases. Caution should therefore be

used when selecting an HIV-1 integrase enzymatic system for drug screening. It should also be kept in mind when interpreting structural studies that at least one of the two mutated residues (F185K) is present in every crystal structure obtained so far (Dyda et al., 1994; Goldgur et al., 1998, 1999; Maignan et al., 1998; Chen et al., 2000a; Wang et al., 2001).

Finally, relative activity in the presence of Mg^{2+} and relative activity in the wild-type enzyme seem also to correlate with antiviral activity. DA-DKA (Zhang et al., 2002), MA-DKA (Zhang et al., 2002), and L-708,906 (Hazuda et al., 2000; Pais et al., 2002) are potent antiviral compounds, whereas 5CITEP, DKA1, and DKA2 (Pais et al., 2002) are not antiviral. If this trend is confirmed for larger compound sets, the sensitivity of a compound against wild-type enzyme versus the F185K/C280S double-mutant, and the selectivity toward Mg^{2+} versus Mn^{2+}, may be an outright indicator for in vivo activity.

References

Allen FH and Kennard O (1993) Three-D search and research using the Cambridge Structural Database. *Chem Design Automation News* **8:**1, 31–37.

Bao KK, Wang H, Miller JK, Erie DA, Skalka AM, and Wong I (2003) Functional oligomeric state of avian sarcoma virus integrase. *J Biol Chem* **278:**1323–1327.

Billich A (2003) S-1360 Shionogi-GlaxoSmithKline. *Curr Opin Investig Drugs* **4:**206–209.

Bischerour J, Leh H, Deprez E, Brochon JC, and Mouscadet JF (2003) Disulfide-linked integrase oligomers involving c280 residues are formed in vitro and in vivo but are not essential for human immunodeficiency virus replication. *J Virol* **77:**135–141.

Bock CW, Kaufman Katz A, Markham GD, and Glusker JP (1999) Manganese as a replacement for magnesium and zinc: functional comparison of the divalent ions. *J Am Chem Soc* **121:**7360–7372.

Bowerman B, Brown PO, Bishop JM, and Varmus HE (1989) A nucleoprotein complex mediates the integration of retroviral DNA. *Genes Dev* **3:**469–478.

Brooks BR, Bruccoleri RE, Olafson BD, States DJ, Swaminathan S, and Karplus M (1983) CHARMM: a program for macromolecular energy, minimization and dynamics calculations. *J Comput Chem* **4:**187–217.

Brown PO (1998) Integration, in *Retroviruses* (Coffin JM, Hughes SH and Varmus HE eds) pp 161–203, Cold Spring Harbor Laboratory Press, Cold Spring Harbor, NY.

Cai M, Zheng R, Caffrey M, Craigie R, Clore GM, and Gronenborn AM (1997) Solution structure of the N-terminal zinc binding domain of HIV-1 integrase. *Nat Struct Biol* **4:**567–577.

Chen JC, Krucinski J, Miercke LJ, Finer-Moore JS, Tang AH, Leavitt AD, and Stroud RM (2000a) Crystal structure of the HIV-1 integrase catalytic core and C-terminal domains: a model for viral DNA binding. *Proc Natl Acad Sci USA* **97:**8233–8238.

Chen Z, Yan Y, Munshi S, Li Y, Zugay-Murphy J, Xu B, Witmer M, Felock P, Wolfe A, Sardana V, et al. (2000b) X-ray structure of simian immunodeficiency virus integrase containing the core and C-terminal domain (residues 50–293)—an initial glance of the viral DNA binding platform. *J Mol Biol* **296:**521–533.

Cherepanov P, Maertens G, Proost P, Devreese B, Van Beeumen J, Engelborghs Y, De Clercq E, and Debyser Z (2003) HIV-1 integrase forms stable tetramers and associates with LEDGF/p75 protein in human cells. *J Biol Chem* **278:**372–381.

De Clercq E (2001) New developments in anti-HIV chemotherapy. *Curr Med Chem* **8:**1543–1572.

Deprez E, Tauc P, Leh H, Mouscadet JF, Auclair C, and Brochon JC (2000) Oligomeric states of the HIV-1 integrase as measured by time-resolved fluorescence anisotropy. *Biochemistry* **39:**9275–9284.

Dyda F, Hickman AB, Jenkins TM, Engelman A, Craigie R, and Davies DR (1994) Crystal structure of the catalytic domain of HIV-1 integrase: similarity to other polynucleotidyl transferases. *Science (Wash DC)* **266:**1981–1986.

Engelman A and Craigie R (1992) Identification of conserved amino acid residues critical for human immunodeficiency virus type 1 integrase function in vitro. *J Virol* **66:**6361–6369.

Engelman A and Craigie R (1995) Efficient magnesium-dependent human immunodeficiency virus type 1 integrase activity. *J Virol* **69:**5908–5911.

Esposito D and Craigie R (1998) Sequence specificity of viral end DNA binding by HIV-1 integrase reveals critical regions for protein-DNA interaction. *Embo Journal* **17:**5832–5843.

Farnet CM and Haseltine WA (1991) Determination of viral proteins present in the human immunodeficiency virus type 1 preintegration complex. *J Virol* **65:**1910–1915.

Foloppe N and MacKerell ADJ (2000) All-Atom Empirical Force Field for Nucleic Acids: I. Parameter Optimization Based on Small Molecule and Condensed Phase Macromolecular Target Data. *J Comput Chem* **21:**86–102.

Gao K, Butler SL, and Bushman F (2001) Human immunodeficiency virus type 1 integrase: arrangement of protein domains in active cDNA complexes. *EMBO (Eur Mol Biol Organ) J* **20:**3565–3576.

Goldgur Y, Craigie R, Cohen GH, Fujiwara T, Yoshinaga T, Fujishita T, Sugimoto H, Endo T, Murai H, and Davies DR (1999) Structure of the HIV-1 integrase catalytic domain complexed with an inhibitor: a platform for antiviral drug design. *Proc Natl Acad Sci USA* **96:**13040–13043.

Goldgur Y, Dyda F, Hickman AB, Jenkins TM, Craigie R, and Davies DR (1998) Three new structures of the core domain of HIV-1 integrase: an active site that binds magnesium. *Proc Natl Acad Sci USA* **95:**9150–9154.

Grobler JA, Stillmock K, Hu B, Witmer M, Felock P, Espeseth AS, Wolfe A, Egbertson M, Bourgeois M, Melamed J, et al. (2002) Diketo acid inhibitor mechanism and HIV-1 integrase: implications for metal binding in the active site of phosphotransferase enzymes. *Proc Natl Acad Sci USA* **99:**6661–6666.

Hazuda DJ, Felock P, Witmer M, Wolfe A, Stillmock K, Grobler JA, Espesath A, Gabryelski L, Schlelf W, Blau C, et al. (2000) Inhibitors of strand transfer that prevent integration and inhibit HIV-1 replication in cells. *Science (Wash DC)* **287:**646–650.

Hazuda DJ, Wolfe AL, Hastings JC, Robbins HL, Graham PL, LaFemina RL, and Emini EA (1994) Viral long terminal repeat substrate binding characteristics of the human immunodeficiency virus type 1 integrase. *J Biol Chem* **269:**3999–4004.

Heuer TS and Brown PO (1998) Photo-cross-linking studies suggest a model for the architecture of an active human immunodeficiency virus type 1 integrase-DNA complex. *Biochemistry* **37:**6667–6678.

Jenkins TM, Engelman A, Ghirlando R, and Craigie R (1996) A soluble active mutant of HIV-1 integrase: involvement of both the core and carboxyl-terminal domains in multimerization. *J Biol Chem* **271:**7712–7718.

Johnson AA, Marchand C, and Pommier Y (2003) HIV-1 integrase inhibitors: a decade of research and two drugs in clinical trial. *Curr Top Med Chem,* in press.

Jorgensen WL, Chandrasekhar J, Madura JD, Impey RW, and Klein ML (1983) Comparison of simple potential functions for simulating liquid water. *J Chem Phys* **79:**926–935.

Jorgensen WL, Maxwell DS, and Tirado-Rives J (1996) Development and testing of the OPLS all-atom force field on conformational energetics and properties of organic liquids. *J Am Chem Soc* **118:**11225–11236.

Karki RG, Tang Y, and Nicklaus M (2002) Model of the HIV-1 Integrase-viral DNA complex—a template for structure-based design of HIV integrase inhibitors, in Proceedings of the 223rd National Meeting of the American Chemical Society; 2002 Apr 7–11; Orlando, FL.

King PJ, Lee DJ, Reinke RA, Victoria JG, Beale K, and Robinson WE Jr (2003) Human immunodeficiency virus type-1 integrase containing a glycine to serine mutation at position 140 is attenuated for catalysis and resistant to integrase inhibitors. *Virology* **306:**147–161.

Leh H, Brodin P, Bischerour J, Deprez E, Tauc P, Brochon JC, LeCam E, Coulaud D, Auclair C, and Mouscadet JF (2000) Determinants of Mg^{2+}-dependent activities of recombinant human immunodeficiency virus type 1 integrase. *Biochemistry* **39:**9285–9294.

Lodi PJ, Ernst JA, Kuszewski J, Hickman AB, Engelman A, Craigie R, Clore GM, and Gronenborn AM (1995) Solution structure of the DNA binding domain of HIV-1 integrase. *Biochemistry* **34:**9826–9833.

MacKerell AD Jr, Bashford D, Bellott M, Dunbrack RL Jr, Evanseck JD, Field MJ, Fischer S, Gao J, Guo H, Ha S, et al. (1998) All-atom empirical potential for molecular modeling and dynamics studies of proteins. *J Phys Chem B* **102:**3586–3616.

Maignan S, Guilloteau JP, Zhou-Liu Q, Clement-Mella C, and Mikol V (1998) Crystal structures of the catalytic domain of HIV-1 integrase free and complexed with its metal cofactor: high level of similarity of the active site with other viral integrases. *J Mol Biol* **282:**359–368.

Marchand C, Neamati N, and Pommier Y (2001) In vitro human immunodeficiency virus type 1 integrase assays. *Methods Enzymol* **340:**624–633.

Marchand C, Zhang X, Pais GC, Cowansage K, Neamati N, Burke TR Jr, and Pommier Y (2002) Structural determinants for HIV-1 integrase inhibition by beta-diketo acids. *J Biol Chem* **277:**12596–12603.

Miller MD, Farnet CM, and Bushman FD (1997) Human immunodeficiency virus type 1 preintegration complexes: studies of organization and composition. *J Virol* **71:**5382–5390.

Neamati N (2002) Patented small molecule inhibitors of HIV-1 integrase: a 10-year saga. *Expert Opin Ther Patents* **12:**709–724.

Pais GC, Zhang X, Marchand C, Neamati N, Cowansage K, Svarovskaia ES, Pathak VK, Tang Y, Nicklaus M, Pommier Y, et al. (2002) Structure activity of 3-aryl-1, 3-diketo-containing compounds as HIV-1 integrase inhibitors. *J Med Chem* **45:**3184–3194.

Podtelezhnikov AA, Gao K, Bushman FD, and McCammon JA (2003) Modeling HIV-1 integrase complexes based on their hydrodynamic properties. *Biopolymers* **68:**110–120.

Pommier Y, Pilon AA, Bajaj K, Mazumder A, and Neamati N (1997) HIV-1 integrase as a target for antiviral drugs. *Antiviral Chem Chemother* **8:**463–483.

Priet S, Navarro JM, Querat G, and Sire J (2003) Reversion of the lethal phenotype of an HIV-1 integrase mutant virus by overexpression of the same integrase mutant protein. *J Biol Chem*

Richman DD (2001) HIV chemotherapy. *Nature (Lond)* **410:**995–1001.

Singh SB, Zink DL, Bills GF, Teran A, Silverman KC, Lingham RB, Felock P, and Hazuda DJ (2003a) Four novel bis-(naphtho-gamma-pyrones) isolated from *Fusarium* species as inhibitors of HIV-1 integrase. *Bioorg Med Chem Lett* **13:**713–717.

Singh SB, Zink DL, Dombrowski AW, Polishook JD, Ondeyka JG, Hirshfield J, Felock P, and Hazuda DJ (2003b) Integracides: tetracyclic triterpenoid inhibitors of HIV-1 integrase produced by *Fusarium* sp. *Bioorg Med Chem* **11:**1577–1582.

Skalka AM (1999) *Retroviral Integration.* Academic Press, San Diego.

Sotriffer CA, Ni H, and McCammon JA (2000a) Active site binding modes of HIV-1 integrase inhibitors. *J Med Chem* **43:**4109–4117.

Sotriffer CA, Ni H, and McCammon JA (2000b) HIV-1 integrase inhibitor interac-

tions at the active site: prediction of binding modes unaffected by crystal packing. *J Am Chem Soc* **122:**6136–6137.
Wang JY, Ling H, Yang W, and Craigie R (2001) Structure of a two-domain fragment of HIV-1 integrase: implications for domain organization in the intact protein. *EMBO (Eur Mol Biol Organ) J* **20:**7333–7343.
Witvrouw M, Fikkert V, Van Maele B, Pannecouque C, Neamati N, Burke TR, Pais G, De Clercq E, and Debyser Z (2002) Antiviral resistance to diketo acids is associated with mutations T66I, L74M and S230R in the HIV integrase Gene presented at the 15th International Conference on Antiviral Research, Prague, Czech Republic. *Antiviral Res* **53:**A18.
Yoshinaga T, Fujishita T, and Fujiwara T (2002) In vitro activity of new HIV-1 integrase inhibitors in clinical development, in 9th Conference on Retroviruses and Opportunistic Infections; 2002 Feb 24–28; Seattle, WA.
Young SD and the HIV integrase inhibitor discovery team (2002) L-870,810: A potent antiviral HIV integrase inhibitor with potential clinical utility XIV International AIDS Conference; 2002 Jul 7–12; Barcelona, Spain.
Zagarian L, Benleulmi MS, Renisio JG, Merad H, Maroun RG, Wieber F, Mauffret O, Porumb H, Troalen F, and Fermandjian S (2003) Strategy to discriminate between high and low affinity bindings of human immunodeficiency virus, type 1 integrase to viral DNA. *J Biol Chem* **278:**19966–19973.
Zhang X, Pais GC, Svarovskaia ES, Marchand C, Johnson AA, Karki RG, Nicklaus MC, Pathak VK, Pommier Y, and Burke TR (2003) Azido-containing aryl beta-diketo acid HIV-1 integrase inhibitors. *Bioorg Med Chem Lett* **13:**1215–1219.
Zhao L, O'Reilly MK, Shultz MD, and Chmielewski J (2003) Interfacial peptide inhibitors of HIV-1 integrase activity and dimerization. *Bioorg Med Chem Lett* **13:**1175–1177.
Zhuang L, Wai JS, Embrey MW, Fisher TE, Egbertson MS, Payne LS, Guare JP Jr, Vacca JP, Hazuda DJ, Felock PJ, et al. (2003) Design and synthesis of 8-hydroxy-[1,6]naphthyridines as novel inhibitors of HIV-1 integrase in vitro and in infected cells. *J Med Chem* **46:**453–456.

Address correspondence to: Dr. Yves Pommier, Laboratory of Molecular Pharmacology, Center for Cancer Research, Bldg. 37, Rm. 5068, National Cancer Institute, National Institutes of Health, Bethesda, MD 20892-4255. E-mail: pommier@nih.gov